Comparative Experimental Evaluation of Conventional Solar Still (CSS) and CSS Augmented with Wax Filled Metallic Finned-Cups

Pankaj Dumka

Assistant professor
Department of mechanical engineering
Jaypee University to Engineering &
Technology,A.B. Road, Guna-473226,
Madhya Pradesh
India

Dhananjay R. Mishra

Assistant professor
Department of mechanical engineering
Jaypee University to Engineering &
Technology,A.B. Road, Guna-473226,
Madhya Pradesh
India

Dwindling potable water is a big concern for the whole world in general and developing nations in particular. Solar still is found to be suitable for the production of potable water at low cost, especially in the arid regions. In view to improve the distillate output of the solar still, the augmentation of the sensible and latent heat, a storage material was needed. For the purpose, wax filled metallic finned cups were used. In this paper, an attempt was made to investigate (experimentally and theoretically) the performance of a conventional solar still integrated with wax filled metallic finned-cups (MSS). Outdoor experiments were conducted on conventional solar still (CSS) and CSS augmented with wax filled metallic finned-cups, in the month of January and February 2019, at Raghogarh, Guna (24°39'N, 77°19'E, India). Linear regression model proposed by Kumar and Tiwari was used to evaluate the performance of solar stills. An improvement of 15.63 and 16.95% in evaporative and convective heat transfer coefficients (from water to condensing cover) have been observed in MSS, as compared with the CSS respectively. It was found that the overall efficiency of MSS increased by 24.64% in compared with the CSS.

Keywords: Desalination, Solar still, Heat storage material, Energy analysis.

1. INTRODUCTION

Water is one of the essential commodities needed for the survival of human beings on the earth. Expeditious industrialization and population growth have led to the serious problem of water stress, as our natural water resources are now entered an epoch of paucity. According to the world water council report [1], the global average per person availability of renewable water resource is going to reduce from 6600 to 4800 m^3 during 2000-2025. Although many methods like reverse osmosis [2], film distillation [3] etc. are available for converting brackish water into potable water, but poor and developing nations lack the skills and fund to deploy them. So to solve this problem of water crisis, solar still is recognized long back as a simple low cost device. The first use of solar still has reported way back in 1872 by Wilson [4], for supplying potable water to the nitrate mining society. Later on many engineers and researchers have worked on these basin-type solar stills which are commonly known as conventional solar stills (CSS) [5,6]. A CSS has low distillate output and requires large surface area for mass production. With this background, various researchers have proposed different methodology for enhancing the productivity of passive distiller units [7–16].

Jamil and Akhtar [17] reported the influence of characteristic length of solar still cavity (aspect ratios from 1.94 to 2.67) on the distillate yield. A detailed theoretical analysis of different climatic parameters on the productivity of CSS have been reported by Afrand and Karimpour [18].

An improvement in distillate yield by augmenting still with earth has been reported by Sodha et al. [19]. Dumka and Mishra [20] have reported a detailed energy and exergy analysis of single basin solar still integrated with the earth surface. Effect on distillate yield by covering nearby ground of sand bed solar still with polythene sheet and coal powder have been reported by Tiwari and Mishra [21]. Using ANN model a hybrid solar distiller unit integrated with an air compressor has been reported by Hidouri et al. [22]. Rabhi et al. [23] have reported the augmentation of fins (in basin area) and external condenser with the solar still. Dumka et al. [24] have experimentally examined the use of permanent ferrite ring magnets for magnetizing the brackish water in conventional solar still. They have reported a substantive increase in the distillate output and efficiency of still augmented with magnets.

Kalidasa et al. [25] have observed that the use of rubber in the basin area of still can enhance the evaporation rate and distillate output. Exergy and economic analysis of CSS integrated with rectangular porous media have been reported by Rashidi et al. [26]. Mishra and Tiwari [27] have reported an enhancement of distillate yield by spreading coal and metal chips within the basin area. Ibrahim et al. [28] have given a comprehensive review on absorption energy storage using (with and without) crystallization of the absorption materials for single and multi effect distiller

units. A comprehensive review on an application of nano-fluids in solar stills have been reported by Khanafer and Vafai [29]. Deshmukh and Thombre [30] have reported the use of sand and servo-therm medium oil beneath the basin liner, as sensible heat storage material. Dumka et al. [31]have reported the influence of salt concentration on the internal heat transfer coefficients and efficiency of a CSS.

Gugulothu et al. [32] have reported an experimental study on the performance of a single basin solar still by using potassium dichromate, magnesium sulphate hepta-hydrate and sodium acetate as an energy storage materials. They observed that magnesium sulphate hepta-hydrate gives better distillate output as compared to others. Kabeel et al. [33] have delineated a comparative study of experimental and exergy analysis of a passive water desalination system, with and without paraffin wax as phase change material in the basin and parabolic concentrator. They have observed that PCM and parabolic concentrator augmented still produces 55-65% and 35-45% higher yield than the conventional still. Arunkumar et al. [34] examined the effect of carbon impregnated foam (CIF) and bubble-wrap (BW) insulation on distillate output of single slope solar still having basin area of $0.5m^2$, and have validated their CFD results with the experiments. They reported an increment of 21.05%, 63.16% and 15.79% in distillate output by using, BW insulation, BW insulation & CIF and saw dust respectively in CSS as compared to CSS alone. Kabeel et al. [35] reported a comparative theoretical study among different organic and inorganic PCM along with their economic analysis. They have observed that Capric-Palmatic (inorganic) and A48 (organic) have the combined advantage of high yield and low cost, but A48 has an edge over the Capric-Palmatic as it is environment friendly. A comparative study of three stills i.e. CSS, CSS with sensible heat energy storage, and CSS with jute knitted sensible energy storage under different water mass have been reported by Kabeel et al.[35]. They have observed that for 20 kg of water, jute knitted sensible energy storage still yields 18% more than the still with only sensible energy storage material.

In this communication, an attempt was made to determine the effect of wax filled finned-cup (that are supposed to act as sensible and as latent heat storage material) on the internal heat transfer coefficients, distillate yield and efficiency of a conventional solar still. Experimental data obtained by the outdoor experimentations in the month of January and February 2019 were evaluated using, model proposed by Kumar and Tiwari. It waas observed that still containing wax filled metallic-finned cups gives very high nocturnal yield and hence, high distillate output and efficiency.

2. EXPERIMENTAL SETUP

For experimentation, two identical single slope conventional solar still (CSS) are fabricated with the help of 5 mm thick FRP material keeping 1 m² basin area, with lower and higher vertical sides of 0.48 and 0.2 m heights respectively. For better absorption of solar energy,

inner surface of stills were painted with the black colour. Solar stills are covered with iron transparent glass of 4 mm thickness, at an inclination of 15.6º with reference to horizontal surface.

As water wets the glass surface, so the condensation of vapours on it will obviously be film condensation. But it has been proved by Bhardwaj et al. [36] that the film condensation allow more solar radiation to pass through them when compared to dropwise condensation, and hence film condensation results better yield in solar still. Recently Arunkumar et al. [34] have shown that the use of bubble wrap insulation can reduce the heat loss from side and bottom considerably. So, both the stills were insulated form sides and bottom with bubble wrap. The schematic arrangement, and actual photograph of CSS are shown in Figure 1 and 2 respectively.
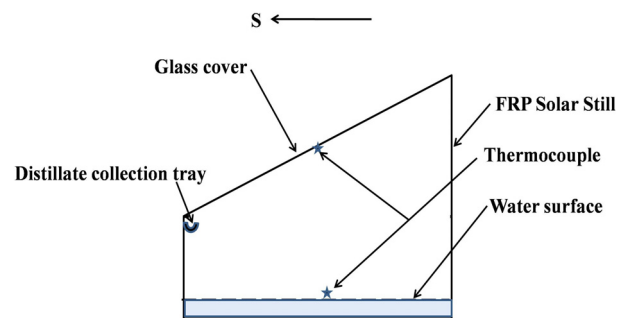

Figure 1. Schematic of CSS [20]

Figure 2. Photograph of CSS

To enhance the productivity of CSS twelve wax filled, finned cylindrical cups (Figure 3) of 6 cm height and 8 cm inner diameter were placed within the solar still at equal distance (to ensure maximum absorption of incident radiation, minimum wall shadow effect, and equal heat dissipation within the basin area), as shown in the Figure 5.

Each cup contains 44 mm long, and 2 mm diameter fins, painted with black colour to ensure the maximum absorption and radiation from Sun to energy storage material (during charging), and energy storage material to water (during discharging) respectively. Wax is filled till a height of 4 cm in each cup, and the top portion of the cups were sealed with a LLDPE cover (to ensure the isolation of wax from moist air) as shown in Figure 4. The wax used in current study is paraffin wax, whose properties are listed in Table 1.

Figure 3. Photograph of finned cup with wax

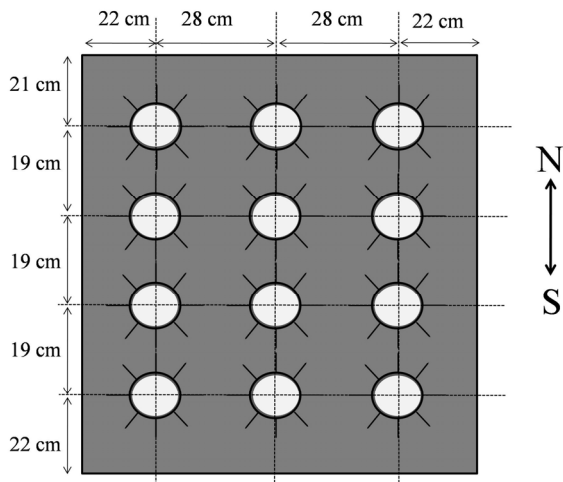**Figure 4. Photograph of finned cup with wax covered with LLDPE**

Figure 5. Arrangement of finned cups in the basin area of still

Table 1. Thermophysical properties of wax [37]

Property	Value in SI units
Density	in liquid state [760 (kg/m³)]
	in solid state [818 (kg/m³)]
Latent heat of fusion	226 (kJ/kg)
Melting temperature	56ºC
Thermal conductivity	0.24 [W/(mK)]
Specific heat capacity	in solid state [2.95 (kJ/(kgK))]
	in liquid state [2.51 (kJ/(kgK))]

The photograph of Modified Solar Still (MSS), i.e. the CSS augmented with wax filled finned cups is shown in Figure 6.

Figure 6. Photograph of finned cup with wax covered with LLDPE

Five K-type thermocouples (K 7/32-2C-TEF) were deployed in the still for the measurement of atmospheric, inner glass, outer glass, water, and basin temperatures in CSS, whereas six thermocouples are deployed in MSS. Different temperatures were recorded with the help of DTC324A-2 temperature indicator during the experimentation. LX-107 solar power meter has been used to measure incident solar radiation during the experimentation. For the measurement of distillate output a graduated cylinder has been used respectively. Photo graph of full experimental setup is shown in Figure 7.

Figure 7. Photograph of finned cup with wax covered with LLDPE

In the experimentations it is assumed that the data is distributed uniformly so, Type B uncertainties are considered. In this type, the standard uncertainty is evaluated as [38]:

$$u = a / \sqrt{3} \tag{1}$$

where, a is the accuracy of the measuring instrument. Table 2 represents the accuracy, range, and standard uncertainty of the measuring instruments.

Each experimental run is of 48 h time duration.

Thirty kg of brackish water is maintained in the basin area of solar still throughout the experimentation. Following observations were made during experiments:

- Atmospheric, basin, water, inner glass, outer glass, and finned cup temperatures.
- Intensity of incident solar radiation on inclined glass cover.

- Distillate output at an interval of one hour.

Table 2. Accuracy, range and standard uncertainties of measuring devices

Instrument	Accuracy	Range	Standard Uncertainty
Solar Power meter	±10 W/m^2	0-1999 W/m^2	5.77 W/m^2
Thermocouple	±0.1ºC	-100-100ºC	0.06ºC
Graduated Cylinder	±1 ml	0 - 250 ml	0.6 ml

3. MATHEMATICAL BACKGROUND

To understand the physics behind a particular thermodynamic system, one should always write the governing equations which can define the system holistically. For the solar still in current study, following assumptions are considered to develop the energy balance equations:

- Leak proof solar still.
- Side, and bottom heat loss from still are neglected.
- The water, glass, basin, and finned-cup temperatures have very insignificant variation spatially.
- System is in quasi-equilibrium condition between two successive readings during the course of time.
- Wax filled metallic finned-cup is considered as one combined system. This is in immediate consequence of third assumption.
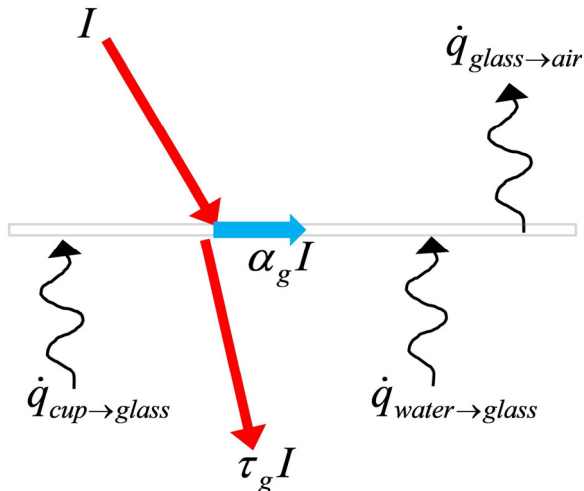- Neglecting the shadow effect.

3.1 Solar still with finned-cup (MSS)

Based on the above mentioned assumptions, energy balance equations for different sections of MSS can be written as follows:

3.1.1 Glass cover

Based on the Figure 8, the energy equation is as follows:

$$(h_{rg} + h_{cg})A_g(T_{ci} - T_a) = I\alpha_g A_g + h_{1w}(T_w - T_{ci})A_w + (h_{c\to g}^{rad} + h_{c\to g}^{conv})(T_c - T_{ci})A_c^{ETA}$$
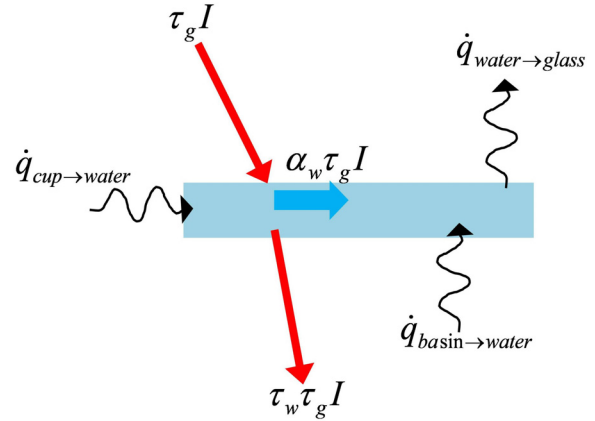
Figure 8. Energy balance of glass cover with finned-cup

3.1.2 Saline water
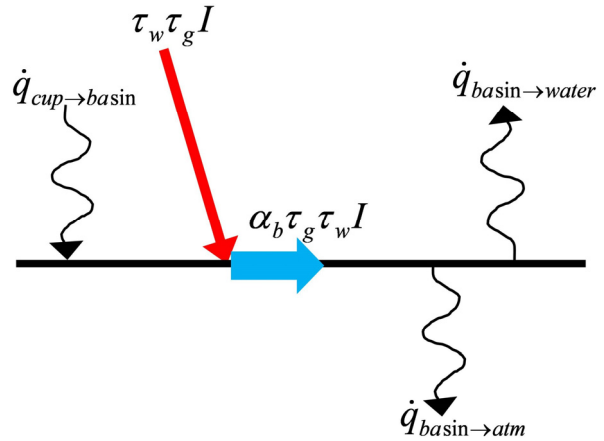
Based on the Figure 9 the energy equation is as follows:

$$(MC)_w \frac{dT_w}{dt} = \alpha_w \tau_w IA_w + h_1(T_b - T_w)A_b + h_{c\to w}^{conv}(T_c - T_w)A_c^{ETW} - h_{1w}(T_w - T_{ci})A_w$$

Figure 9. Energy balance of saline water with finned-cup

3.1.3 Basin liner

Based on the Figure 10 the energy equation is as follows:

Figure 10. Energy balance of basin liner with finned-cup

$$\alpha_b \tau_g \tau_w IA_b + h_{c\to b}^{cond}(T_c - T_b)A_c^{base} = h_1(T_b - T_w)A_b$$

where, $\dot{q}_{bain\to atm} = 0$ (because of second assumption).

3.1.4 Finned-Cup

Based on the Figure 11 the energy equation is as follows:

$$(MC)_c \frac{dT_c}{dt} = \alpha_{cup}\tau_g IA_c^{ETW} - (h_{c\to g}^{rad} + h_{c\to g}^{conv})(T_c - T_{ci})A_c^{ETA} - h_{c\to w}^{conv}(T_c - T_w)A_c^{ETA} - h_{c\to b}^{cond}(T_c - T_w)A_c^{base}$$

Above equations are for the case when the cup is discharging (i.e. gaining energy from incident solar radiations) of cup the direction of energy interactions from cup just changes their sign, and rest of the equations mentioned above will remain same.
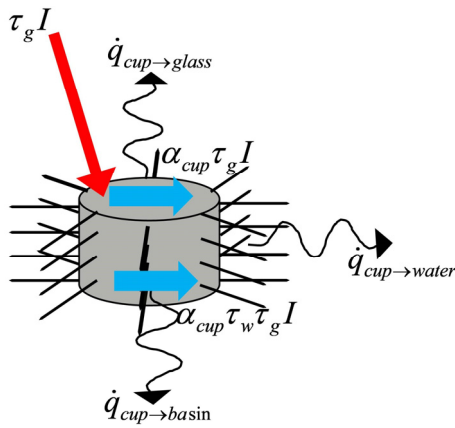
Figure 11. Energy balance of finned-cup

3.2 Solar still without finned-cup (CSS)

3.2.1 Glass cover

Based on the Figure 12, the energy equation is as follows:

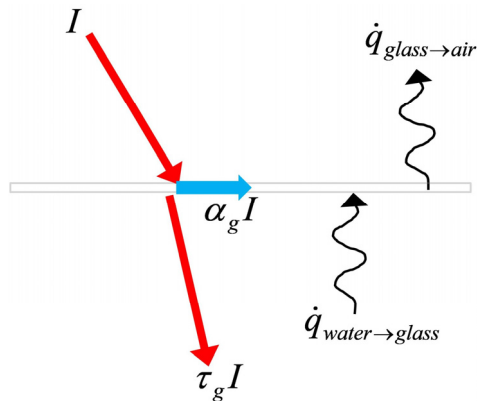$$(h_{rg} + h_{cg})A_g(T_{ci} - T_a) = I\alpha_g A_g + h_{1w}(T_w - T_{ci})A_w$$

Figure 12. Energy balance of glass cover without finned-cup

3.2.2 Saline water

Based on the Figure 13 the energy equation is as follows:

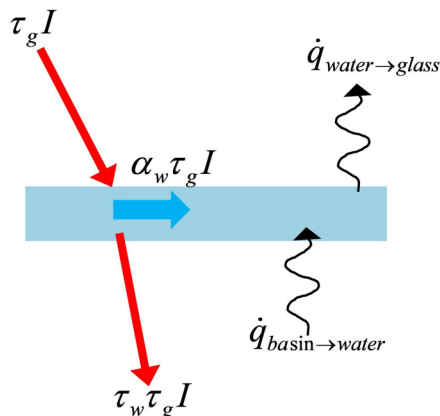$$(MC)_w \frac{dT_w}{dt} = \alpha_w \tau_w IA_w + h_1(T_b - T_w)A_b + h_{1w}(T_w - T_{ci})A_w$$

Figure 13. Energy balance of basin water without finned cup

3.2.3 Basin liner

Based on the Figure 14, the energy equation is as follows:

$$\alpha_b \tau_g \tau_w IA_b = h_1(T_b - T_w)A_b$$

The convective heat transfer rate is proportional to the temperature difference of water and glass, and the constant of proportionality is convective heat transfer coefficient, as written below:

$$\dot{q}_{cw} = h_{cw}(T_w - T_{ci})$$

Grashof number (Gr) infer the flow regime in the cases where fluid motion is solely caused by natural convection currents. The relation between Nu, Gr, and Pr number is as follows :

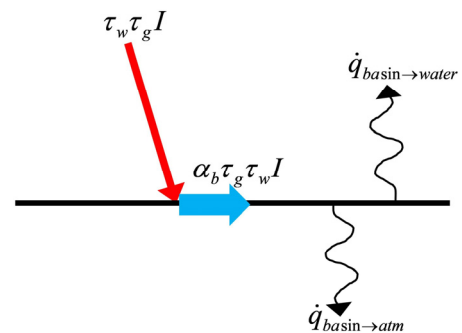$$Nu = \frac{h_{cw}d}{k} = C(Gr.\text{Pr})^n$$

Figure 14. Energy balance of basin liner without finned-cup

The thermo-physical properties of moist air are calculated using property relations reported by Tsilingiris [39]. Numerical values of C and n are required to evaluate h_{cw}. Many theoretical models are there to calculate the numerical magnitude of C and n. For theoretical analysis, authors have used the model proposed by Kumar and Tiwari [40] in this manuscript, which is based on linear regression analysis, as it is not limited to Gr range. It takes in the distillate yield, solar radiation intensity, water, glass and ambient air temperatures as an input, and returns the values of C and n as output. The values of C and n from this model are as follows:

$$n = \frac{N\sum xy - \sum x \sum y}{N\sum x^2 - (\sum x)^2}$$

$$C = \exp\left(\frac{\sum y - n\sum x}{N}\right)$$

Once h_{cw} is known h_{ew} can be evaluated as [40]:

$$h_{ew} = 0.016273 \times h_{cw}\frac{P_w - P_{ci}}{T_w - T_{ci}}$$

thereafter, the theoretical distillate yield can be written as:

$$\dot{m}_{ew} = \frac{h_{ew}(T_w - T_{ci}) \times 3600}{L}$$

The radiative heat transfer coefficient from water to inner glass surface is evaluated as follows [20]:
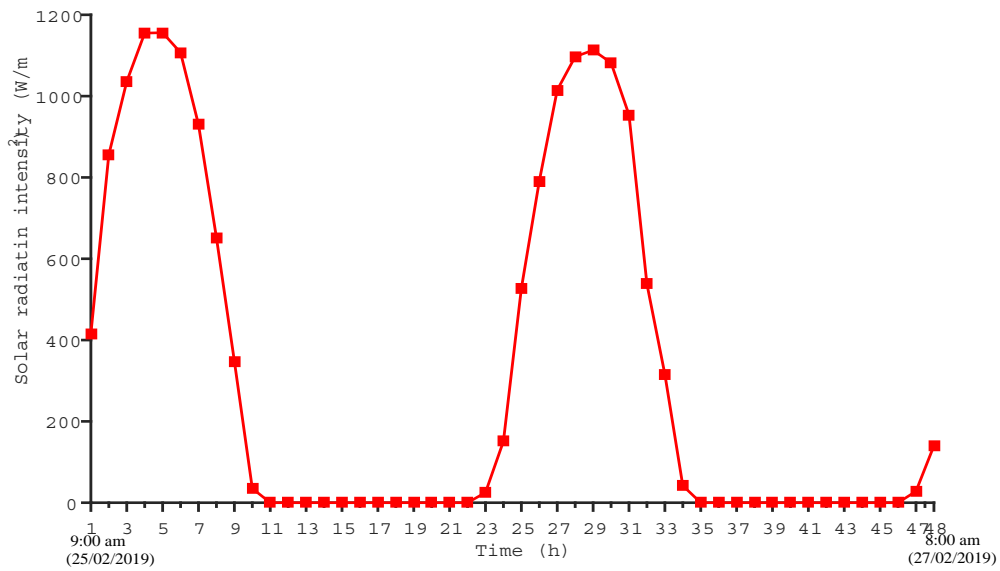
Figure 15. Variation of solar radiation intensity on glass cover as a function of time
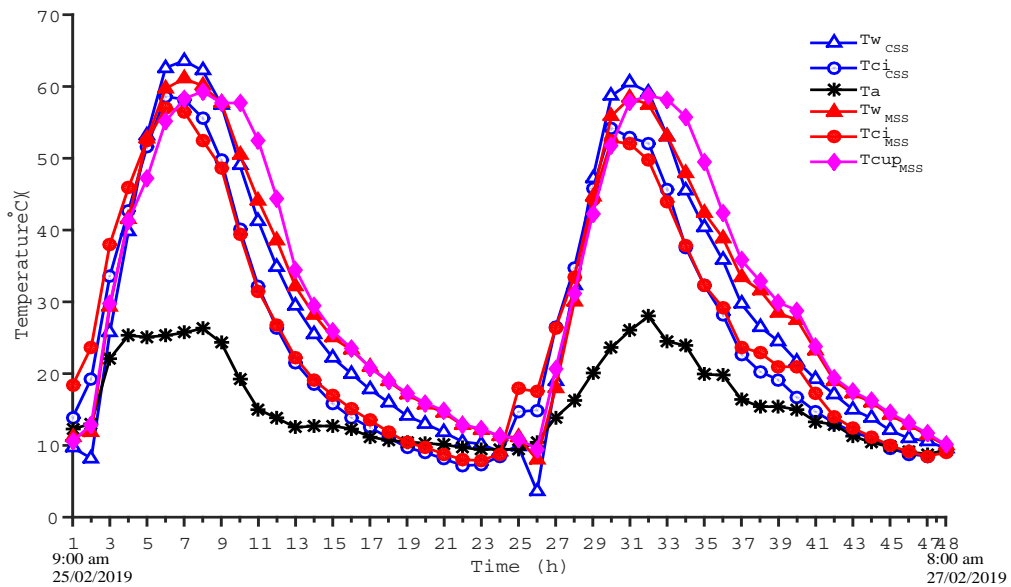
Figure 16. Variation of ambient, water, inner glass and finned-cup temperatures as a function of time
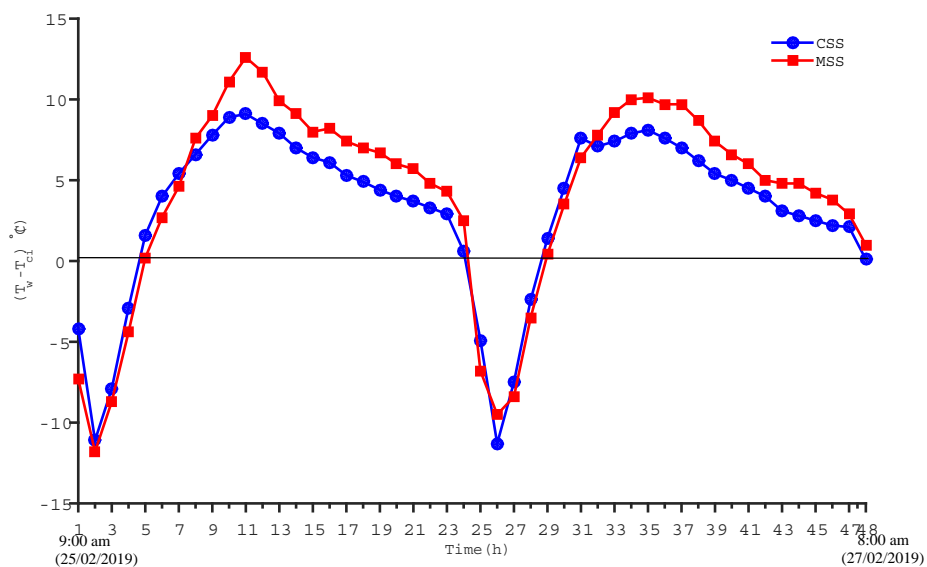
Figure 17. Variation of water and inner glass temperature difference as a function of time

Figure 18. Variation of evaporative heat transfer coefficient as a function of time

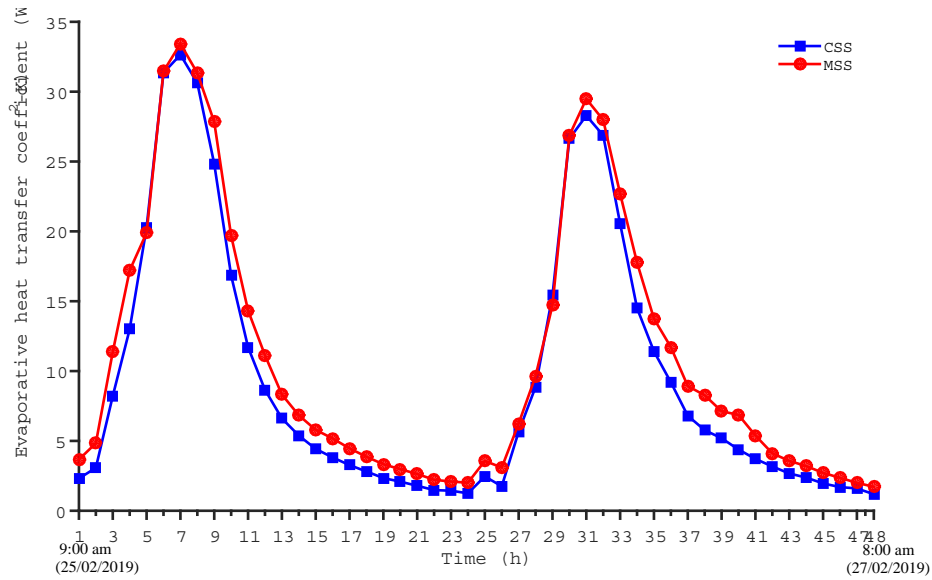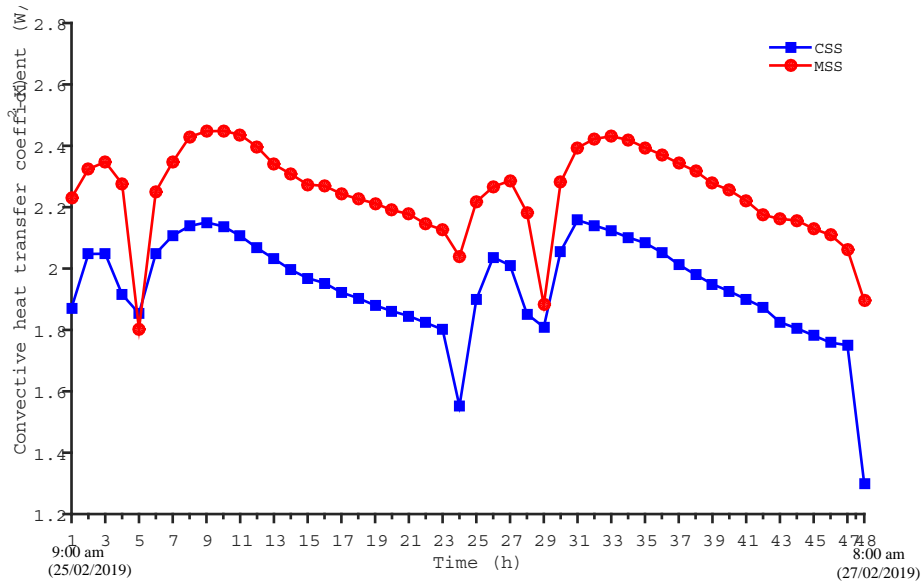**Figure 19. Variation of evaporative heat transfer coefficient as a function of time**
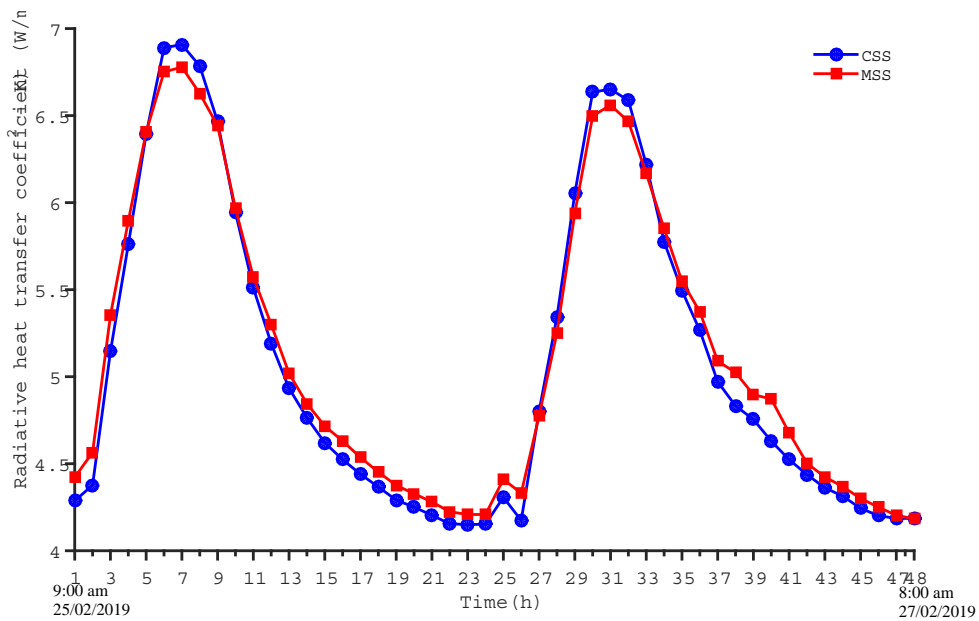

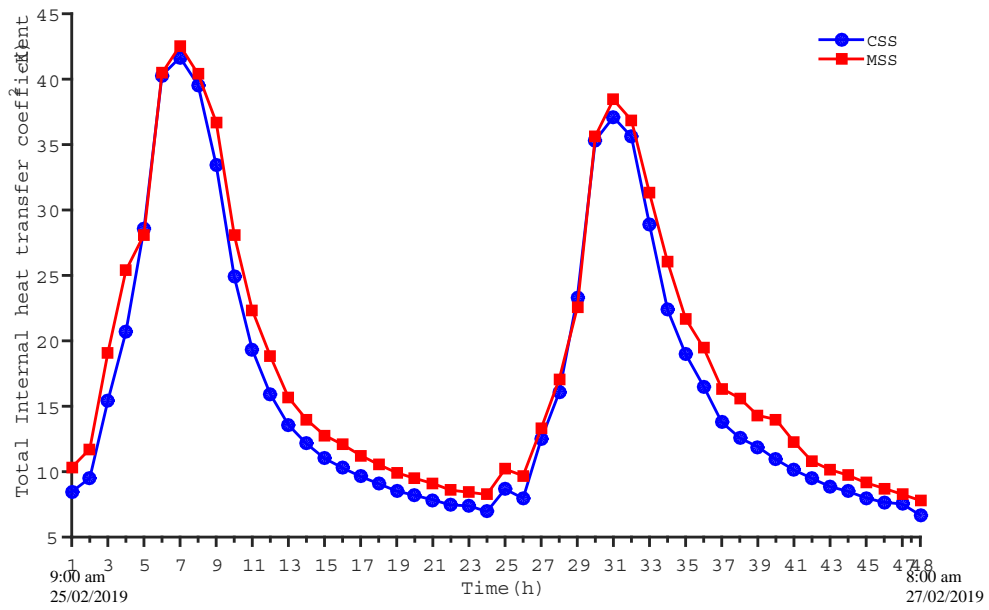**Figure 20. Variation of radiative heat transfer coefficient as a function of time**

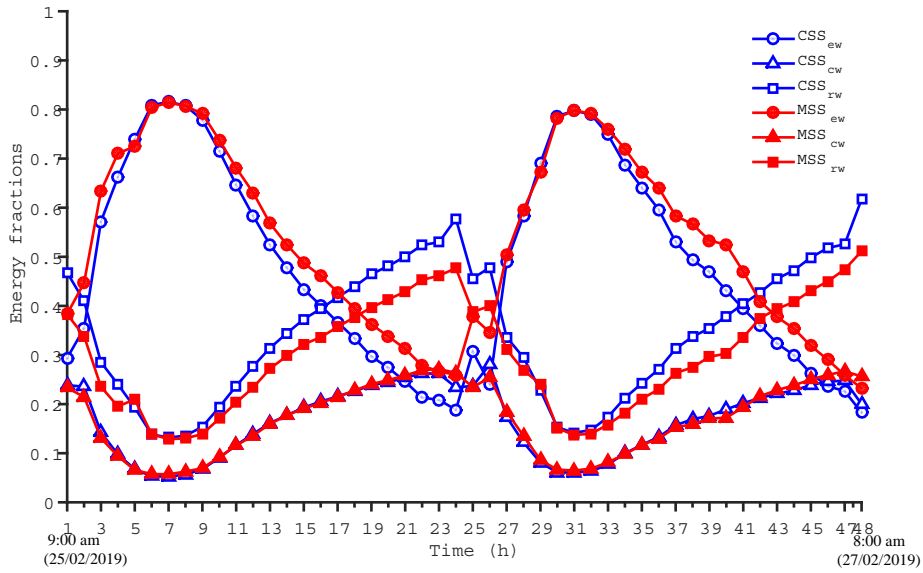**Figure 21. Variation of overall heat transfer coefficient as a function of time**

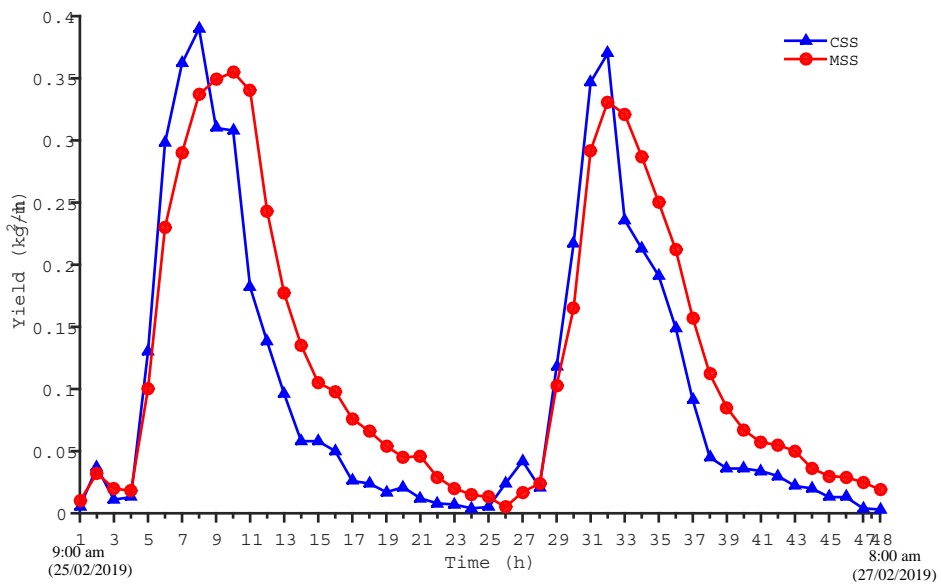**Figure 22. Variation of energy fractions as a function of time**

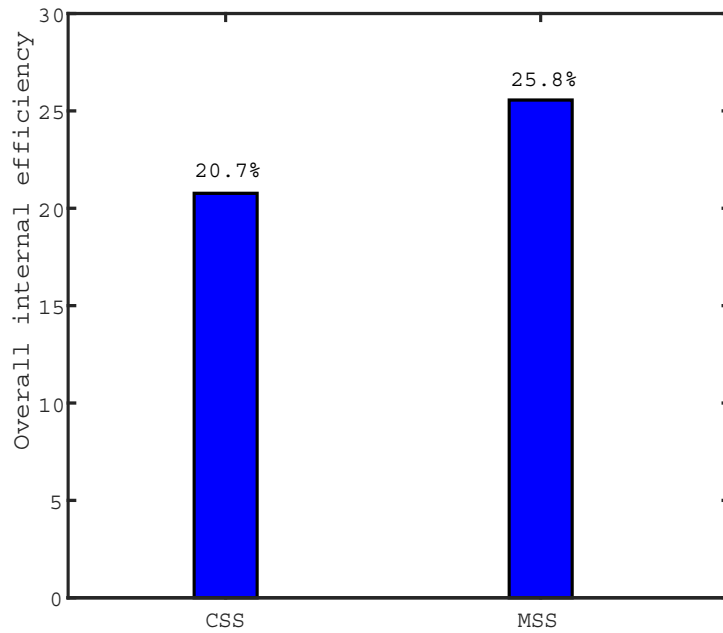**Figure 23. Variation of yield as a function of time**

Figure 24. Overall internal efficiency for CSS and MSS

$$h_{rw} = \varepsilon_{eff} \times \sigma \times \left((T_w + 273.15)^2 + (T_{ci} + 273.15)^2 \right) \times$$
$$(T_w + T_{ci} + 546.2)$$

where, $\dfrac{1}{\varepsilon_{eff}} = \dfrac{1}{\varepsilon_w} + \dfrac{1}{\varepsilon_{ci}} - 1$

The overall heat transfer rate from water to inner glass surface can be written as:

$$\dot{q}_{water \to glass} = \dot{q}_{ew} + \dot{q}_{cw} + \dot{q}_{rw} = h_{1w} \times (T_w - T_{ci})$$

Energy fractions, which can be used to find out the most influential mode of heat transfer within the still, and are evaluated as follows:

$$F_{ew} = \dot{q}_{ew} / \dot{q}_{water \to glass}; F_{cw} = \dot{q}_{cw} / \dot{q}_{water \to glass};$$
$$F_{rw} = \dot{q}_{rw} / \dot{q}_{water \to glass}$$

The overall efficiency of a solar still is defined as the ratio of thermal energy required to obtain a specific amount of distillate output to that of total solar energy as input, and mathematically it is written as [20]:

$$\eta_i = \frac{\sum (\dot{m}_{ew} \times L)}{\sum (I(t) \times A_w \times 3600)} \times 100$$

4. OBSERVATIONS, RESULTS AND DISCUSSION

Figure 15 shows the variation of solar radiation intensity with respect to time during the experimentation. For the first day (i.e. 25/02/2019), at the start of the experiment, the solar radiation recorded was 416 W/m², which attains a maximum value of 1156 W/ W/m² at 13:00 h, and decreases to 0 W/m² by 19:00 h. Whereas, the maximum values of incident solar radiations recorded on the second day (26/02/2019) of continuous experimentation was 1113 W/m² at 13:00 h. Thereafter it reduces and attains a minimum value of 0 W/m² by 19:00 h and maintains it till next day morning

(27/02/2019). At the end of the experiment (8:00 h) the recorded solar radiation intensity was 140 W/m².

Figure 16 shows the hourly variation of ambient, water, inner glass, and wax filled finned-cup tempe- ratures for CSS and MSS. At the start of the experiment (i.e. at 9:00 h on 25/02/2019), the condensing cover temperature has been recorded as 43.3 and 65.8% higher than the basin water temperature, for CSS and MSS respectively. Whereas for the next day (26/02/2019), at the same time inner glass temperature shows an upsurge of 50 and 61.2% over water temperature for CSS and MSS respectively. For both the days, after 12:00 h, the water temperature takes the lead and maintains it throughout the experimentation till 8:00 h next day. For CSS, the maximum recorded water temperatures are 63.6ºC (first day) and 60.5ºC (second day) at 15:00 h, which are 9.28 and 14.37% higher than the inner condensing temperature respectively, at ambient tempe- rature of approximately 26ºC. Whereas for MSS, the maximum water temperatures recorded (at 15:00 h) are 61.1ºC (first day) and 58.4ºC (second day), which are 8.14 and 12.31% higher than the inner glass temperature respectively. The reason for water to attain the highest temperature 2 h later (at 15:00 h) than the maximum solar radiation (at 13:00 h) is that: the heat capacity of water (in CSS), and water & wax filled finned cups (in MSS) will not allow water to increase its temperature instantaneously with the solar radiation. It is seen that finned cup temperature (T_c) increases with time due to the increased heat transfer rate by convection from the surrounding water and solar radiations to the finned cup as the solar radiation intensity increases. The wax started to melt after 6 h (at 15:00 h), from the beginning of still exposure to solar radiation, for both the days. Subsequently, T_c remains nearly constant until it melts completely; then, it decreases slowly with time after sunset when the discharging process of the energy stored by the wax begins. However, the temperatures of the basin water and glass cover of the still decrease much faster with time due to decrease in the ambient

temperature. This causes a significant temperature difference between water and cup till late night for both dates. By looking at the trend it is eminent that from 9:00 h till 18:00 h the finned-cup is charging and then it discharges its energy to the water.

Figure 17 shows the variation of ΔT throughout the experiment for both the stills (i.e. MSS and CSS). It is apparent that during morning hours glass receives the radiation first and its temperature increases faster in contrast to the temperature rise of water which results in negative ΔT. The ΔT remains negative till water temperature does not overtake glass temperature. The Maximum positive temperature difference of 12.6 and 12.1ºC has been recorded between water and inner glass at 15:00h for MSS whereas, for CSS it is 9.1 and 8.1ºC at 19:00 h for first and second consecutive days respectively.

The variation of evaporative heat transfer coefficient with respect to time for MSS and CSS is shown in Figure 17. It has been observed that MSS leads CSS throughout the experimentation except at 13:00 h where CSS leads MSS marginally by 2 and 4.4% for day one (25/02/2019) and two (26/02/2019) respectively. The reason for this rise may be the ΔT (Figure 16), which is just crossing the zero line for MSS at 13:00 h. Augmenting CSS with the finned cups (MSS) has lead to an appreciable improvement in h_{ew} from 14:00 h till 8:00 h next day, for both the days. On first day, at 9:00 h, h_{ew} evaluated for MSS is 59.13% higher than that of CSS. MSS maintains its lead till 12:00 h but, at 13:00 h CSS take over MSS as this is the time when ΔT cross over zero line. Thereafter, h_{ew} for MSS takes its lead over CSS and attains a maximum value of 32.65 W/m²K at 15:00 h. From 15:00 h till 10:00 h on second day, MSS maintains its lead, thereafter CSS takes over MSS till 14:00 h. The maximum value of h_{ew} attained by MSS on second day was 29.48 W/(m²K) at 15:00 h. After 15:00 h till the end of experimentation, similar trend has been observed. Over all, there has been an improvement of 15.63% in the value of h_{ew} for MSS in comparison to CSS.

The variation of convective and radiative heat transfer coefficients for CSS and MSS are shown in Figure 19 and 20 respectively. There has been a significant improvement in the value of h_{ew} due to presence of wax filled finned cups. For both CSS and MSS a sharp discontinuity in the nature can be seen at points 5, 24, 29 and 48, this is due to the very small value (very much close to zero) of ΔT at these points. Maximum value of h_{cw} for MSS is obtained at 18:00 h in both the days, where MSS leads CSS by 31.09 and 31.78% for day one (25/02/2019) and day two (26/02/2019) respectively. Augmenting CSS with wax filled metallic finned-cups have improved the h_{cw} for MSS by 16.95% over CSS. During the experimentation it has been observed that average value of h_{rw} for MSS leads over CSS by 1.3%.

As already discussed in equation 17, the overall heat transfer coefficient is the cumulative impact of evaporative, convective, and radiative heat transfer coefficients. So, to understand the behaviour of total heat transfer from water to glass, Figure 21 depicts its variation as a function of time. At 9:00 h, h_{1w} evaluated for MSS are 21.9 and 17.7% higher than CSS for day one

(25/02/2019) and day two (26/02/2019) respectively. The maximum values of h_{rw} evaluated for MSS are 42.56 and 38.44 W/m²K at 15:00 h for day one and day two respectively. After 24 h for both days the value of h_{rw} for MSS leads CSS by 17.3 and 27.9% respectively for day one and two respectively. The average value of h_{rw} for MSS is evaluated to be 11.7% higher than CSS.

Energy fraction has been calculated based on equation 19, and their variation as function of time is shown in Figure 22. The maximum contribution is of evaporative heat transfer coefficient, followed by radiative, and least contribution is of convective heat transfer coefficient. The augmentation of finned-cups to CSS have a considerable improvement in the evaporative and radiative energy fractions (as these are the only dominating mode of energy transfer in still). After 1:00 h in the night for both the days, the evaporative and radiative energy fractions change their nature: due to decreasing temperature difference between water and glass temperatures.

For 48 h observation, the distillate yield recorded from MSS is 22.44 % higher than CSS viz. 5.932 l/m². Figure 23 shows the variation of distillate yield from CSS and MSS as a function of time. Table 3 gives the comparative view of cumulative yield recorded during the shine and the off-shine hours for day one and two (from 9:00 h (25/02/2019) till 6:00 h (27/02/2019)).

Table 3. Cumulative Distillate yield (in ml) recorded at shine and off-shine hours for day one and two

Type of still	Day one		Day two	
	Day	Nocturnal	Day	Nocturnal
CSS	1864	690	1604	680
MSS	1741	1414	1593	1140

From Table 3 it is clear that the distillate yield recorded during day time (shine hours) is slightly lower for MSS whereas, for night time (off shine hours) it is much higher for MSS in comparison to CSS. For day one the recorded distillate yield for MSS lags by 7.06% during shine hours and leads by 104.92% during off-shine hours in comparison to CSS. Whereas for the second day, the MSS lags by 0.7% during shine hours and leads by 67.65% during off-shine hours in comparison to CSS. The higher value of distillate output in night time is due to the energy discharging from the wax filled-finned cups.

Figure 24 shows a bar graph which depicts the overall efficiency of CSS and MSS during 48 h of experimentation. It shows that the augmentation of CSS with the wax filled metallic finned-cups has considerably improved the overall efficiency of MSS by 24.64% in compared to CSS.

5. CONCLUSION

Two identical conventional solar stills were experimentally and numerically investigated under Guna (24º39'N, 77º19'E, India) weather conditions. Twelve wax filled metallic finned-cups were placed in one still (called MSS) to enhance the internal heat transfer coefficients along with distillate output. Experiments were carried out for continuous 48 h, with different experimental sets spread over the month of January and February of 2019. On the basis of experimental and

theoretical analysis of CSS and MSS, following conclusions can been drawn:

- Distillate output of MSS is enhanced by 22.44% due to the augmentation of wax filled metallic finned-cups.

- During nocturnal hours the distillate yield recorded from MSS is higher by 104.92 and 67.65% in comparison to CSS for day one (25/02/2019) and day two (26/02/2019) respectively (due to the presence of wax filled finned-cups covered with LLDPE) .

- The average evaporative heat transfer coefficient from water to inner condensing cover of MSS has been evaluated as 15.63% higher as compared to CSS.

- It has been observed that the convective heat transfer coefficient from water to inner condensing cover of MSS improved by 16.95% as compared with the CSS.

- The augmentation of wax filled metallic finned-cups with the CSS has improved the internal efficiency by 24.64%

ACKNOWLEDGMENT

REFERENCES

[1] WWC. No Title. 2017.

[2] Wenten IG, Khoiruddin. Reverse osmosis applications: Prospect and challenges. Desalination 2016. doi:10.1016/j.desal.2015.12.011.

[3] Alkhudhiri A, Darwish N, Hilal N. Membrane distillation: A comprehensive review. Desalination 2012;287:2–18. doi:10.1016/J.DESAL.2011.08.027.

[4] Tiwari GN, Tiwari AK. Solar Distillation Practice for Water Desalination Systems. New Delhi, India: Anamaya; 2008.

[5] Kabeel AE, El-Agouz SA. Review of researches and developments on solar stills. Desalination 2011;276:1–12. doi:10.1016/j.desal.2011.03.042.

[6] Ayoub GM, Malaeb L. Developments in solar still desalination systems: A critical review. Crit Rev Environ Sci Technol 2012;42:2078–112. doi:10.1080/10643389.2011.574104.

[7] Tiwari AK, Tiwari GN. Effect of water depths on heat and mass transfer in a passive solar still: in summer climatic condition. Desalination 2006;195:78–94. doi:10.1016/j.desal.2005.11.014.

[8] Dwivedi VK, Tiwari GN. Comparison of internal heat transfer coefficients in passive solar stills by different thermal models: An experimental validation. Desalination 2009;246:304–18. doi:10.1016/j.desal.2008.06.024.

[9] Taghvaei H, Taghvaei H, Jafarpur K, Karimi Estahbanati MR, Feilizadeh M, Feilizadeh M, et al. A thorough investigation of the effects of water depth on the performance of active solar stills. Desalination 2014;347:77–85. doi:10.1016/j.desal.2014.05.038.

[10] Rahmani A, Boutriaa A, Hadef A. An experimental approach to improve the basin type solar still using an integrated natural circulation loop. Energy Convers Manag 2015;93:298–308. doi:10.1016/j.enconman.2015.01.026.

[11] Shafii MB, Favakeh A, Faegh M, Sadrhosseini H. Experimental investigation of a novel passive solar still with additional condensation on sidewalls. Desalin Water Treat 2017. doi:10.5004/dwt.2017.21334.

[12] Omara ZM, Abdullah AS, Kabeel AE, Essa FA. The cooling techniques of the solar stills' glass covers – A review. Renew Sustain Energy Rev 2017;78:176–93. doi:10.1016/j.rser.2017.04.085.

[13] Tanaka H. A theoretical analysis of basin type solar still with flat plate external bottom reflector. Desalination 2011;279:243–51. doi:10.1016/j.desal.2011.06.016.

[14] Xiao G, Wang X, Ni M, Wang F, Zhu W, Luo Z, et al. A review on solar stills for brine desalination. Appl Energy 2013;103:642–52. doi:10.1016/j.apenergy.2012.10.029.

[15] Selvaraj K, Natarajan A. Factors influencing the performance and productivity of solar stills - A review. Desalination 2018;435:181–7. doi:10.1016/j.desal.2017.09.031.

[16] Sharon H, Reddy KS. A review of solar energy driven desalination technologies. Renew Sustain Energy Rev 2015. doi:10.1016/j.rser.2014.09.002.

[17] Jamil B, Akhtar N. Effect of specific height on the performance of a single slope solar still: An experimental study. Desalination 2017;414:73–88. doi:10.1016/j.desal.2017.03.036.

[18] Afrand M, Karimipour A. Theoretical analysis of various climatic parameter effects on performance of a basin solar still. J Power Technol 2017; 97: pp. 44–51.

[19] Sodha MS, Mishra DR, Tiwari AK. Solar Earth Water Still for Highly Wet Ground. J Fundam Renew Energy Appl 2014;4:1–2. doi:10.4172/2090-4541.1000e103.

[20] Dumka P, Mishra DR. Energy and exergy analysis of conventional and modified solar still integrated with sand bed earth: Study of heat and mass transfer. Desalination 2018;437:15–25. doi:10.1016/j.desal.2018.02.026.

[21] Tiwari AK, Mishra DR. Effect of covering by blak polythene sheet and coal powder on near by surfaces of sand bed solar still : Studying heat and mass transfer. 10th Int. Conf. Heat Transf. Fluid Mech. Thermodyn., 2014.

[22] Hidouri K, Mishra DR, Benhmidene A, Chouachi B. Experimental and theoretical evaluation of a hybrid solar still integrated with an air compressor using ANN. Desalin WATER Treat 2017;88:52–9. doi:10.5004/dwt.2017.21333.

[23] Rabhi K, Nciri R, Nasri F, Ali C, Bacha H Ben. Experimental performance analysis of a modified single-basin single-slope solar still with pin fins absorber and condenser. Desalination 2017;416:86–93. doi:10.1016/j.desal.2017.04.023.

[24] Dumka P, Kushwah Y, Sharma A, Mishra DR. Comparative analysis and experimental evaluation of single slope solar still augmented with permanent magnets and conventional solar still. Desalination 2019;459:34–45. doi:10.1016/j.desal.2019.02.012.

[25] Kalidasa Murugavel K, Chockalingam KKSK, Srithar K. Progresses in improving the effectiveness of the single basin passive solar still. Desalination 2008;220:677–86. doi:10.1016/j.desal.2007.01.062.

[26] Rashidi S, Rahbar N, Sadegh M, Abolfazli J. Enhancement of solar still by reticular porous media : Experimental investigation with exergy and economic analysis. Appl Therm Eng 2018;130: 1341–8. doi:10.1016/j.applthermaleng.2017.11.089.

[27] Mishra DR, Tiwari AK. Effect of coal and metal chip on the solar still. J Sci Tech Res 2013;3:1–6.

[28] Ibrahim NI, Al-Sulaiman FA, Ani FN. Solar absorption systems with integrated absorption energy storage–A review. Renew Sustain Energy Rev 2018;82:1602–10. doi:10.1016/j.rser.2017.07.005.

[29] Khanafer K, Vafai K. A review on the applications of nanofluids in solar energy field. Renew Energy 2018; 123:398–406. doi:10.1016/j.renene.2018.01. 097.

[30] Deshmukh HS, Thombre SB. Solar distillation with single basin solar still using sensible heat storage materials. Desalination 2017;410:91–8. doi:10.1016/j.desal.2017.01.030.

[31] Dumka P, Mishra DR. Influence of salt concentration on the performance characteristics of passive solar still. Int J Ambient Energy 2019:1–11. doi:10. 1080/01430750.2019.1611638.

[32] Gugulothu R, Somanchi NS, Devi RSR, Banoth HB. Experimental Investigations on Performance Evaluation of a Single Basin Solar Still Using Different Energy Absorbing Materials. Aquat Procedia 2015; Vol. 4: pp. 1483–91. doi:10.1016/j.aqpro.2015.02.192.

[33] Kabeel AE, Elkelawy M, Alm H, Din E, Alghrubah A. Investigation of exergy and yield of a passive solar water desalination system with a parabolic concentrator incorporated with latent heat storage medium. Energy Convers Manag 2017;145:10–9. doi:10.1016/j.enconman.2017.04.085.

[34] Arunkumar T, Kabeel AE, Raj K, Denkenberger D, Sathyamurthy R, Ragupathy P, et al. Productivity enhancement of solar still by using porous absorber with bubble-wrap insulation. J Clean Prod 2018; Vol. 195: 1149–61. doi:10.1016/j.jclepro.2018.05.199.

[35] Kabeel AE, El-Samadony YAF, El-Maghlany WM. Comparative study on the solar still performance utilizing different PCM. Desalination 2018;432:89–96. doi:10.1016/j.desal.2018.01.016.

[36] Bhardwaj R, ten Kortenaar M V., Mudde RF. Influence of condensation surface on solar distillation. Desalination 2013;326:37–45. doi:10.1016/j.desal.2013.07.006.

[37] A.A. El-Sebaii, A.A. Al-Ghamdi, F.S. Al-Hazmi ASF. Thermal performance of a single basin solar still with PCM as a storage medium. Appl Energy 2009; Vol. 86: pp. 1187–95. doi:10.1016/j.apenergy.2008.10.014.

[38] Abolfazli J, Rahbar N, Lavvaf M. Utilization of thermoelectric cooling in a portable active solar still - An experimental study on winter days. DES 2011; 269:198–205. doi:10.1016/j.desal.2010.10 .062.

[39] Tsilingiris PT. The influence of binary mixture thermophysical properties in the analysis of heat and mass transfer processes in solar distillation systems. Sol Energy 2007;81:1482–91. doi:10.1016/j.solener.2007.02.005.

[40] Kumar S, Tiwari GN. Estimation of convective mass transfer in solar distillation systems. Sol Energy 1996;57:459–64. doi:10.1016/S0038-092X(96)00122-3.

NOMENCLATURE

A_b	basin area (m^2)
A_c^{base}	total area of cups exposed to basin (m^2)
A_c^{ETA}	total area of cups exposed to air (m^2)
A_c^{ETW}	total area of cups exposed to water (m^2)
A_g	glass cover area (m^2)
A_w	evaporative surface area (m^2)
c_p	specific heat capacity at constant pressure (J/kg K)
C	constant
d	characteristic length of solar still (m^2)
F_{cw}	convective heat transfer fraction
F_{ew}	evaporative heat transfer fraction
F_{rw}	radiative heat transfer fraction
g	acceleration due to gravity (m/s^2)
Gr	Grashof number
h_{cg}	convective heat transfer coefficient from glass to air (W/(m^{2}K))
h_{cw}	convective heat transfer coefficient from water to glass (W/(m^{2}K))
$h_{c \to b}^{cond}$	conductive heat transfer coefficient from cup to basin (W/(m^{2}K))
$h_{c \to g}^{conv}$	convective heat transfer coefficient from cup to glass (W/(m^{2}K))

$h_{c \to g}^{rad}$	radiative heat transfer coefficient from cup to glass (W/(m^{2}K))
$h_{c \to w}^{conv}$	convective heat transfer coefficient from cup to water (W/(m^{2}K))
h_{ew}	evaporative heat transfer coefficient from water to glass (W/(m^{2}K))
h_{rg}	radiative heat transfer coefficient from glass to air (W/(m^{2}K))
h_{rw}	radiative heat transfer coefficient from water to glass (W/(m^{2}K))
h_1	convective heat transfer coefficient from basin to water (W/(m^{2}K))
h_{1w}	total internal heat transfer coefficient from water to glass (W/(m^{2}K))
$I(t)$	incident solar radiation on inclined cover surface (W/m^2)
k	thermal conductivity of humid air (W/(mK))
L	latent heat of vaporization (J/kg)
$\dot{m}_{ew}$	distillate output (kg/m^{2}h)
$(MC)_w$	heat capacity of water (J/K)
$(MC)_c$	Total heat capacity of wax filled finned cup (J/K)
n	Constant
Nu	Nusselt number
P_{ci}	saturated vapour pressure on inner glass surface (Pa)
P_t	total atmospheric pressure (Pa)
P_w	saturated vapour pressure on water surface (Pa)
Pr	Prandtl number
$\dot{q}_{basin \to air}$	Heat transfer rate from basin to air (W/m^2)
$\dot{q}_{basin \to water}$	Heat transfer rate from basin to water (W/m^2)
$\dot{q}_{cup \to basin}$	Average heat transfer rate from cup to basin (W/m^2)
$\dot{q}_{cup \to glass}$	Average heat transfer rate from cup to glass (W/m^2)
$\dot{q}_{cw}$	Convective heat transfer rate from water to glass (W/m^2)
$\dot{q}_{cup \to water}$	Average heat transfer rate from water to glass (W/m^2)
$\dot{q}_{ew}$	evaporative heat transfer rate from water to glass (W/m^2)
$\dot{q}_{glass \to air}$	Heat transfer rate from glass to air (W/m^2)
$\dot{q}_{rw}$	Radiative heat transfer rate from water to glass (W/m^2)
$\dot{q}_{water \to glass}$	Total heat transfer rate from water to glass (W/m^2)
t	time (s)
T_a	ambient temperature (ºC)
T_c	average temperature of finned-cup (ºC)
T_{ci}	inner glass cover temperate (ºC)
T_v	average temperature of moist air (ºC)
T_w	Temperature of water surface (ºC)
u	Standard Uncertainty

Greek symbols

α_b	absorptivity of basin
α_g	absorptivity of glass
α_w	absorptivity of water
β	expansion factor (K^{-1})
$\Delta T'$	effective temperature difference (ºC)
η_i	instantaneous thermal efficiency
μ	dynamic viscosity of humid air (kg/(ms))
ρ	density of humid air (kg/m^3)
σ	Stefan Boltzmann constant (W/m^{2}K^4)
τ_g	transmissivity of glass
τ_w	transmissivity of water
ε_w	emissivity of water
ε_{ci}	emissivity of glass
ε_{eff}	Effective emissivity

Abbreviations

ANN	artificial neural network
CSS	conventional solar still
FRP	fiber reinforced plastic
LLDPE	linear low density polythene
MSS	modified solar still
PV	photovoltaic

КОМПАРАТИВНА ЕКСПЕРИМЕНТАЛНА ЕВАЛУАЦИЈА КОНВЕНЦИОНАЛНОГ СОЛАРНОГ ДЕСТИЛАТОРА И ДЕСТИЛАТОРА СА ДОДАТНИМ МЕТАЛНИМ РЕБРАСТИМ ШОЉАМА ИСПУЊЕНИХ ВОСКОМ

П. Думка, Д.Р. Мишра

Све мања количина воде за пиће представља велики проблем за цео свет, а посебно за земље у развоју. Соларни дестилатори су погодни за јефтину производњу пијаће воде, нарочито у сушним пределима. Да би се повећала производња пијаће воде у соларним дестилаторима и искористила латентна топлота, био је потребан материјал за складиштење. У ту сврху искоришћене су металне ребрасте шоље испуњене воском.

Рад приказује истраживања (експериментална и теоријска) перформанси конвенционалног соларног дестилатора у који су уграђене металне ребрасте шоље испуњене воском. Пољски експерименти су обављени са оба типа дестилатора (конвенционалним и са додатком) у јануару и фебруару 2019. године у Рагогару, Гуна (24°39' N, 77°19' E) у Индији. Модел линеарне регресије Кумара и Тиварија је коришћен за евалуацију перформанси оба дестилатора.

Утврђен је пораст коефицијената преноса топлоте евапорацијом и конвекцијом од 15,63 до 16,95% код дестилатора са шољама у поређењу са конвен-

ционалним дестилатором. Укупна искоришћеност дестилатора са шољама је порасла за 24,64% у односу на конвенционални дестилатор.